HHS Public Access

Author manuscript

Neurobiol Aging. Author manuscript; available in PMC 2016 June 01.

Published in final edited form as:

Neurobiol Aging. 2015 June ; 36(6): 2010–2017. doi:10.1016/j.neurobiolaging.2015.03.007.

White matter integrity in dementia with Lewy bodies: A Voxel-Based Analysis of Diffusion Tensor Imaging

Zuzana Nedelska, MD[a,h,i], **Christopher G. Schwarz, PhD**[a], **Bradley F. Boeve, MD**[b], **Val Lowe, MD**[a], **Robert I. Reid, PhD**[c], **Scott A. Przybelski**[d], **Timothy G. Lesnick, MS**[d], **Jeffrey L. Gunter, PhD**[c], **Matthew L. Senjem, MS**[c], **Tanis J. Ferman, PhD**[e], **Glenn E. Smith, PhD**[f], **Yonas E. Geda, MD, MS**[g,i], **David S. Knopman, MD**[b], **Ronald C. Petersen, MD, PhD**[b], **Clifford R. Jack Jr., MD**[a], and **Kejal Kantarci, MD, MS**[a,*]

[a]Department of Radiology, Mayo Clinic, Rochester, MN

[b]Department of Neurology, Mayo Clinic, Rochester, MN

[c]Department of Information Technology, Mayo Clinic, Rochester, MN

[d]Department of Health Sciences Research, Mayo Clinic, Rochester, MN

[e]Department of Psychiatry and Psychology, Mayo Clinic, Jacksonville, FL

[f]Department of Psychiatry and Psychology, Mayo Clinic, Rochester, MN

[g]Department of Psychiatry & Psychology, and Department of Neurology, Mayo Clinic, Scottsdale, AZ

[h]Department of Neurology, Charles University in Prague, 2nd Faculty of Medicine and Motol University Hospital, Prague, the Czech Republic

[*]Corresponding Author: Kejal Kantarci MD, MS kantarci.kejal@mayo.edu Phone: 1-507-284 9770 Fax:1-507-284-9778 Mayo Clinic, 200 First Street SW, Rochester, MN 55905, US.

Disclosure Statement: Z. Nedelska, C. Schwarz, R. Reid, S. Przybelski, T. Lesnick, J. Gunter, M. Senjem report no disclosures. B. Boeve has served as an investigator for a clinical trial sponsored by Cephalon, Inc. He has received honoraria from the American Academy of Neurology. He receives research support from the National Institute on Aging (P50-AG16574 [Co-I], U01 AG06786 [Co-I], R01-AG15866 [Co-I], and U24-AG26395 [Co-I]), and the Alzheimer's Association (IIRG-05–14,560 [PI]).T. Ferman is funded by the NIH (Mayo Clinic Alzheimer's Disease Research Center/Project 1-P50-AG16574/P1 [Co-I]). G. Smith is funded by the NIH (P50-AG16574). D. Knopman serves as Deputy Editor for Neurology®; serves on a Data Safety Monitoring Board for Lundbeck Pharmaceuticals and for the Dominantly Inherited Alzheimer's Disease Treatment Unit. He is participating in clinical trials sponsored by Lilly Pharmaceuticals and TauRx Pharmaceuticals. He receives research support from the NIH. R. Petersen serves on scientific advisory boards for Elan Pharmaceuticals, Wyeth Pharmaceuticals, and GE Healthcare and receives research support from the NIH (P50-AG16574 [PI] and U01-AG06786 [PI], R01-AG11378 [Co-I], and U01–24904 [Co-I]). C. Jack serves as a consultant for Janssen, Bristol-Meyer-Squibb, General Electric, Siemens, and Johnson and Johnson and is involved in clinical trials sponsored by Allon and Baxter, Inc. He receives research funding from the National Institutes of Health (R01-AG011378, RO1-AG037551, U01-HL096917, U01-AG032438, U01-AG024904), and the Alexander Family Alzheimer's Disease Research Professorship of the Mayo Foundation Family. K. Kantarci serves on the data safety monitoring board for Pfizer Inc and Takeda Global Research & Development Center, Inc; and she is funded by the NIH (R01AG040042 [PI], P50 AG44170/Project 2 [PI], P50 AG16574/Project 1 [PI], R01 AG11378[Co-I], U19 AG10483[Co-I], U01 AG042791[Co-I]) and Minnesota Partnership for Biotechnology and Medical Genomics (PO03590201[PI]).

[i]International Clinical Research Center, St. Anne's University Hospital Brno, Brno, the Czech Republic

Abstract

Many patients with dementia with Lewy bodies have overlapping Alzheimer's disease (AD)–related pathology, which may contribute to white matter (WM) diffusivity alterations on diffusion tensor imaging (DTI). Consecutive patients with DLB (n=30), age and sex matched AD patients (n=30), and cognitively normal controls (CN; n=60) were recruited. All subjects underwent DTI, 18F 2-fluoro-deoxy-d-glucose (FDG) and 11C Pittsburgh compound B (PiB) PET scans. DLB patients had reduced fractional anisotropy (FA) in the parieto-occipital WM but not elsewhere compared to CN, and elevated FA in parahippocampal WM compared to AD patients, which persisted after controlling for Aβ load in DLB. The pattern of WM FA alterations on DTI was consistent with the more diffuse posterior parietal and occipital glucose hypometabolism of FDG PET in the cortex. DLB is characterized by a loss of parieto-occipital WM integrity, independent of concomitant AD-related Aβ load. Cortical glucose hypometabolism accompanies WM FA alterations with a concordant pattern of gray and white matter involvement in the parieto-occipital lobes in DLB.

Keywords

dementia with Lewy bodies; diffusion tensor imaging; white matter integrity; amyloid-beta load; voxel-based analysis; cortical hypometabolism

1. Introduction

Diffusion tensor imaging (DTI) provides information on white matter (WM) microstructure, utilizing the anisotropic nature of water diffusion, which is impeded perpendicularly to WM fibers. Fractional anisotropy (FA) is a robust DTI-derived measure (Pierpaoli and Basser, 1996) of the directionality of water diffusion, which decreases with the degeneration of WM. Hence, FA is often used as a proxy of WM integrity (Carmichael and Lockhart, 2012; Douaud et al., 2011).

DTI studies in dementia with Lewy bodies (DLB) have reported varying extents of white matter (WM) involvement, ranging from wide-spread reduced FA in the corpus callosum, frontal, parietal, occipital and temporal WM (Bozzali et al., 2005; Lee et al., 2010), to involvement confined to temporo-parietal limbic and occipital pathways (Firbank et al., 2007; Firbank et al., 2011; Kiuchi et al., 2011; Watson et al., 2012). Reduced FA in the occipital WM, specifically in the inferior longitudinal fasciculus, a pathway important for visuo-spatial processing, was a common finding in DLB patients (Bozzali et al., 2005; Kantarci et al., 2010; Kiuchi et al., 2011; Lee et al., 2010; Ota et al., 2008; Watson et al., 2012). Many DLB patients who fulfill the clinical criteria for probable DLB have overlapping Alzheimer's disease (AD)–related pathology, which may have contributed to the variation in WM diffusivity alterations in DLB.

^{11}C Pittsburgh compound B (PiB) on PET imaging traces β-amyloid (Aβ) plaques which are present in both AD and LB dementias (Rowe et al., 2007 ;Foster et al., 2010). Although PiB binds to Aβ in both the neuritic and diffuse plaques (Klunk et al., 2001; Mathis et al., 2002), it has a higher affinity to neuritic plaques. Further, PiB does not bind to α-synuclein in Lewy bodies. (Burack et al., 2010; Fodero-Tavoletti et al., 2007; Kantarci et al., 2012c). Therefore, PiB uptake on PET can serve as a marker of AD-related Aβ pathology in DLB.

18F 2-fluoro-deoxy-glucose (FDG) PET findings in DLB are characterized by hypometabolism in the occipital and posterior temporo-parietal cortex (Imamura et al., 1997; Minoshima et al., 2001). However, cortical atrophy has not been observed in these posterior brain regions, neither in cross-sectional MRI studies in clinically-diagnosed DLB patients, (Middelkoop et al., 2001; Whitwell et al., 2007), nor in a longitudinal MRI study that investigated the pattern of cortical atrophy rates on antemortem MRI in an autopsy-confirmed cohort (Nedelska et al., 2014). Because DLB patients show a specific pattern of reduced cortical metabolism, FDG PET is particularly useful to examine the neurodegenerative changes in the cortical gray matter, and to assess whether hypometabolism in the cortex relates to a loss of WM integrity in DLB.

It remains unknown whether or not AD-related Aβ pathology is responsible for the alterations in WM microstructure in patients with DLB. Further, it is unclear whether the WM alterations on DTI topographically coincide with cortical hypometabolism observed on FDG PET in DLB. First, we determined the pattern of WM diffusivity alterations in DLB compared to cognitively normal controls and AD patients using voxel-based analysis across the WM of the entire brain. Second, we examined the contribution of Aβ load to the disruption of WM integrity in patients with DLB, and finally we compared the pattern of WM alterations on DTI and cortical glucose hypometabolism on FDG PET in DLB.

2. Methods

2.1. Subjects and Clinical Evaluations

We identified thirty consecutive patients with probable DLB (McKeith et al., 2005) from a prospective, longitudinally followed cohort at the Mayo Clinic Alzheimer's Disease Research Center (ADRC; a dementia clinic-based cohort) in Rochester, MN during a three-year period 2010 – 2013. For comparison, we included thirty patients with probable AD (McKhann et al., 1984) and sixty cognitively normal controls (CN) either from ADRC or from the Mayo Clinic Study on Aging (a community-based cohort) who were matched (1:1 or 2:1, respectively) on age and sex to DLB patients. Eligibility was defined as the absence of any major abnormality on structural MRI that could confound the results such as tumors or large hemispheric infarcts, the absence of primary neurological illness affecting cognition other than DLB or AD, and sufficient scan quality to conduct analysis. The study was approved by the Mayo Clinic Institutional Review Board. All subjects or their proxies provided the informed consent on study participation.

Global measures of Clinical Dementia Rating Sum of Boxes (CDR-SOB; Hughes et al., 1982), Mini Mental State Examination (MMSE; Folstein et al., 1975) and Dementia Rating Scale (DRS; Morris, 1993) were used to assess clinical disease severity at the time of the

study. The presence, duration and severity of DLB clinical features, and the duration of dementia were ascertained. Visual hallucinations (VH) had to be fully formed, recurring, and unlikely to be the consequence of causes other than DLB. VH severity was coded as mild, moderate or severe. Fluctuations were considered present if patients scored 3 or 4 points on the Mayo Clinic Fluctuations questionnaire (Ferman et al., 2004). Motor impairment was scored using motor subscale of the Unified Parkinson's Disease Rating Scale (UPDRS; Fahn, 1987). Probable REM sleep behavior disorder RBD (pRBD) was diagnosed using the International Classification of Sleep Disorders–II diagnostic criteria B for pRBD (AASM, 2005).

2.2. MRI acquisition

MRIs were performed at 3T using an eight channel phased array coil (GE, Milwaukee, WI) and parallel imaging with an acceleration factor of two. A 3D T1-weighted high-resolution magnetization prepared rapid gradient echo acquisition with TR/TE/TI = 7/3/900 ms, flip angle 8 degrees, a slice thickness of 1.2 mm, and in plane resolution of 1.0 mm was obtained for anatomic segmentation and labeling. DTI was acquired using a single-shot echo-planar T2-weighted sequence in the axial plane with the following acquisition parameters: TR = 10,200 ms; in-plane matrix 128/128; FOV 35 cm; phase FOV 0.66. DTI volumes included 41 diffusion-encoding directions, and four non-diffusion weighted T2 images with 2.7 mm slice thickness and 2.7 mm isotropic resolution.

2.3. 11C-PiB and 18F-FDG PET studies

11C-PiB and 18F-FDG PET scans were performed within a median time of seven days before or after DTI. Images were acquired using a PET/CT scanner (DRX, Milwaukee, GE) in 3D on the same day with 1 hour interval between each other. Each subject was injected with 11C PiB and later with 18F-FDG. Following a 40-minutes of PiB uptake period, a 20-min PiB scan consisting of four 5-min dynamic frames was obtained. Following a 30-minute 18F-FDG uptake interval, an 8-minute FDG scan was acquired. PiB and FDG individual scans were affine-coregistered to corresponding T1-weighted MRI scan. PiB and FDG images were parcellated into regions of interest (ROIs) (Tzourio-Mazoyer et al., 2002) using an in-house modified automatic anatomical labelling atlas (Vemuri et al., 2008), and partial volume correction was applied using a brain vs CSF model (Meltzer et al., 1999). The global cortical PiB standardized uptake value ratio (SUVR) was calculated as the median uptake in the bilateral parietal, temporal, prefrontal, orbitofrontal, cingulate precuneus and anterior cingulate cortical uptake divided by uptake in the cerebellar gray matter (Jack et al., 2008). The cortical FDG uptake in each voxel was divided by the median pons FDG uptake. Differences in glucose metabolism between CN and DLB patients were displayed using Statistical Parametric Mapping 5 (SPM5; http://www.fil.ion.ucl.ac.uk/spm), $p<0.001$ and corrected for multiple comparisons using family wise error. W e used pons normalized FDG uptake values from those VBA-derived cortical regions, where FDG uptake was significantly reduced in DLB compared to CN in order to determine the correlations among the focal abnormalities in FDG uptake and DTI findings in DLB.

2.3.3. DTI Analysis—Each of the 41 diffusion-weighted images was affine co-registered to the non-diffusion weighted b0 images to minimize head motion and eddy current-related

distortions. Images were brain-extracted using FSL Brain Extraction Tool (http://fsl.fmrib.ox.ac.uk/fsl/fslwiki/BET). Tensors were fit using a least squares model, and FA maps were generated (Behrens et al., 2003). A voxel-based analysis (VBA) across the whole-brain was conducted using the FA images according to previously-published technique (Schwarz et al., 2014) . Briefly, FA images of all subjects were nonlinearly co-registered via an iterative, group-wise registration algorithm Advanced Normalization Tools (ANTs; Avants et al., 2010) and normalized to a 1 mm isotropic MNI 152 standard space via the FMRIB58_FA template (Jenkinson et al., 2012). The images were smoothed using an 8 mm full-width-half-maximum Gaussian kernel. Non-WM regions were removed by masking out voxels where the mean FA across co-registered subjects' images was < 0.2.

We first examined the topographic pattern of FA differences between each of the two clinical groups on VBA using SPM5 at $p<0.001$ corrected and uncorrected for multiple comparisons to capture the whole range of differences across the DLB spectrum with varying degrees of PiB retention compared to AD and CN groups. Second, we included the individual PiB SUVR as a continuous covariate in regression model to examine the contribution of Aβ load to WM diffusivity alterations in DLB compared to CN. Third, we used FA values from those VBA-derived WM regions, where FA was significantly reduced in DLB compared to CN in order to determine the associations of focal abnormalities in FA with clinical features and focal abnormalities in FDG PET in patients with DLB.

2.4. Statistics

Analyses on subjects' characteristics and correlations were performed using SAS version 9.3 and R statistical software package, version 2.14.0. (http://www.R-project.org) with 2-sided significance set at type I error rate $\alpha < 0.05$. For continuous variables, the medians with interquartile ranges (IQR) were reported along with the p-values from either the Kruskal-Wallis or Wilcoxon two-sample rank sum test. For binary or categorical variables, the proportions (%) were reported along with p-values from X^2 test. The associations between FA values and the duration or severity of clinical features in DLB patients were examined using the Spearman rank correlations.Correlations between duration of visual hallucinations, severity of visual hallucinations, and FA values were determined by likelihood ratio test.

3. Results

3.1. Subjects' characteristics

Subjects' characteristics are listed in **Table 1**. Groups were well matched on sex and age. We treated *APOE* ε4/2 carriers as *APOE* ε4/ε4 or *APOE* ε3/ε4 carriers. The proportion of *APOE* ε4 carriers was highest in AD group ($p<0.001$). Patients with DLB did not differ from AD in the estimated dementia duration ($p=0.88$), or in measures of CDR SOB ($p=0.15$) or MMSE ($p=0.99$). AD patients had a greater Aβ burden than DLB patients ($p<0.001$) on 11C-PiB PET. As expected, the frequencies of VH, pRBD, fluctuations and parkinsonism were higher in DLB compared to AD group ($p<0.001$). Sixteen of the 30 DLB patients (53%) were PiB negative (SUVR<1.5) and 14 (47%) were PiB positive (SUVR≥1.5).

3.2. Patterns of white matter FA alteration on voxel-based analysis

Topographical patterns of between-group differences in FA are displayed in **Figure 1.** We found no differences across the clinical groups after correction for multiple comparisons, therefore we present uncorrected data ($p<0.001$). Patients with AD had markedly reduced FA in temporal and parietal WM and less so in occipital and frontal WM compared to CN. Patients with DLB had FA decreases confined solely to posterior parietal and occipital WM compared to CN. Patients with DLB had a higher FA in the parahippocampal WM compared to AD patients. Median FA values derived from the voxels that have lower FA compared to CN are plotted in **Figure 2** demonstrating that PiB positivity may have influenced the findings, justifying the Aβ load-adjusted analysis.

3.3. Effect of Aβ load on white matter integrity in DLB

Adjustment for Aβ load did not have a substantial effect on the FA alterations in DLB in the parieto-occipital WM. The topographical pattern and magnitude of reduced FA in DLB remained similar between unadjusted and Aβ load-adjusted VBA; the only difference was that the extent of WM involvement shrunk from diffuse parieto-occipital to a well circumscribed area lying on parietal and occipital WM border (**Figure 3**).

3.4. Association of white matter FA alterations with clinical measures in DLB

From DLB-related features, we observed a marginally significant negative association with severity of visual hallucinations (Spearman $r = -0.36$; $p=0.07$) and the parieto-occipital WM FA abnormality on VBA. None of global clinical measures of CDR-SOB, MMSE or DRS correlated with reduced FA in parieto-occipital WM.

3.5. Cortical glucose hypometabolism and white matter FA alterations in DLB

Figure 4 overlays the voxel-based analysis of glucose hypometabolism and FA decreases in patients with DLB compared to the CN group. Patterns of WM alteration and cortical glucose hypometabolism involved similar brain regions in DLB. Although changes on 18F-FDG PET were more diffuse, affecting inferior temporal, posterior parietal and occipital cortices, an overlap with WM FA decreases was obvious in the parieto-occipital lobes. However we did not find an association between parieto-occipital WM FA reduction and cortical glucose metabolism derived from regions that differed from CN subjects on VBA ($p=0.14$).

4. Discussion

This study demonstrates how patients with DLB differ on the pattern of WM integrity disruption from age- and sex-matched CN and AD patients utilizing a voxel-based algorithm examining the white matter of the entire brain. DLB patients are characterized by reduced FA confined to the posterior parietal and occipital WM. Controlling for Aβ load, estimated by a global PiB retention, does not alter this finding and a similar, but more circumscribed pattern of reduced FA is observed in the parietal and occipital WM border in DLB. This suggests WM integrity disruption in this region is only in-part dependent on Aβ load, and is a typical feature of DLB. Comparing the pattern of cortical glucose hypometabolism on 18F-FDG PET and WM FA alterations on DTI, cortical hypometabolic changes were more

wide-spread than WM disruption in DLB. However, these abnormalities overlapped in the parieto-occipital lobes.

In DLB patients, loss of posterior WM integrity has been a consistent finding across a number of DTI studies (Bozzali et al., 2005; Kantarci et al., 2010; Kiuchi et al., 2011; Lee et al., 2010; Ota et al., 2008; Watson et al., 2012) when compared to CN. Whereas we observed reduced FA in the posterior parietal and occipital WM compared to CN, we did not find differences elsewhere, unlike previous studies demonstrating more wide-spread WM involvement of temporal areas (Bozzali et al., 2005; Lee et al., 2010), varying severity of frontal (Bozzali et al., 2005; Lee et al., 2010; Watson et al., 2012) or pontine WM involvement (Watson et al., 2012). Adjustment for Aβ load led to a shrinkage of the regions where posterior parieto-occipital WM FA was significantly reduced, but these were topographically consistent with unadjusted analysis. Patients with DLB commonly have mixed AD pathology, which may be responsible for hippocampal atrophy (Kantarci et al., 2012a; Murray et al., 2013) and greater medial temporal lobe atrophy rates (Nedelska et al., 2014) in these patients. While we do not have autopsy confirmation on a majority of our subjects, adjustment for Aβ load reduced the impact of AD-related pathology on DTI findings. In fact, the occipital FA values derived from the VBA analysis were slightly lower in PiB positive DLB than the PiB negative DLB subjects, although both had reduced FA in this region compared to CN. It is likely that the wide-spread WM involvement in DLB, particularly in the temporal lobes, is associated with mixed AD pathology, which may not be apparent clinically.

Occipital and posterior parietal WM comprise fibers connecting primary and association visual cortices to other brain regions, as well as ‘what’ and ‘where’ distinction pathways (Mesulam, 1998). In keeping with the functional anatomy, and considering that most of our DLB patients had visual hallucinations, an association between visual hallucinations and FA was expected. However, we found only a marginally significant association between FA and the severity of visual hallucinations (coded as mild, moderate or severe). We previously reported an association between presence of visual hallucinations (present vs absent) and reduced FA in the inferior longitudinal fasciculus that connects occipital visual cortex to temporal lobe (Kantarci et al., 2010). It is possible that the relationship between reduced FA and visual hallucinations is confined to the inferior longitudinal fasciculus and not the entire occipital WM FA abnormality we analyzed in this study. Occipital WM has been investigated in autopsy-confirmed cohort DLB patients (Higuchi et al., 2000), where microvacuolation and gliosis were more frequent and severe in the occipital WM in DLB compared to AD patients. Such changes in control brains were minimal. Antemortem occipital hypometabolism on FDG PET characterized those DLB patients with the most severe microvacuolation. Furthermore, microvacuolation was thought to be a substrate for mean diffusivity elevation in the amygdala in DLB (Fujino and Dickson, 2008; Higuchi et al., 2000; Jellinger, 2004; Kantarci et al., 2010). Similarly, WM microvacuolation may be the substrate underlying reduced FA we observed in the parieto-occipital WM of patients with DLB.

We observed that the cortical hypometabolism was largely overlying the disruption in WM integrity in the parieto-occipital lobes. This posterior pattern of glucose hypometabolism,

primarily involving the occipital cortex, is a characteristic feature of DLB (Minoshima et al., 2001) and is independent of AD-related Aβ load (Graff-Radford et al., 2014; Kantarci et al., 2012b). It is thought that the glucose hypometabolism in DLB is related to synaptic dysfunction due to presynaptic α-synuclein deposition with loss of postsynaptic dendritic spines (Kramer and Schulz-Schaeffer, 2007; Zaja-Milatovic et al., 2006), which may contribute to degeneration in the connecting tracts in the WM. Based on this topographic concordance, which was not statistically significant on quantitative analysis, the relationship between reduced WM FA and cortical hypometabolism in the occipital lobe should be further investigated by identifying the cortical connections of WM tracts involved in this region.

When we compared AD patients to CN, we observed reduced FA particularly in the temporo-parietal WM, in agreement with previous DTI studies (Bozzali et al., 2002; Damoiseaux and Greicius, 2009; Huang et al., 2007; Kantarci et al., 2010; Medina et al., 2006; Mielke et al., 2009; Salat et al., 2010). DLB patients had elevated FA in a small but clearly bilateral and symmetric parahippocampal WM compared to AD patients. We found no other differences between these two groups, in agreement with a previous study reporting more asymmetrically reduced FA in the parahippocampal WM in AD patients (Watson et al., 2012). A relative preservation of parahippocampal WM integrity in DLB compared to AD patients is consistent with the preservation of hippocampal volumes on MRI in DLB compared to AD in autopsy-confirmed studies (Burton et al., 2009; Kantarci et al., 2012a; Murray et al., 2013). Dementia duration measured by clinical testing did not differ between our DLB and AD patients, and severity of dementia measured by DRS differed only slightly between these two groups. Our finding suggests that a hippocampal connectivity, which is in part carried by the cingulum tract that runs in the parahippocampal WM, is disrupted in AD but relatively preserved in DLB patients.

A limitation of our study is a lack of autopsy confirmation that could elucidate the role of WM microvacuolation on FA reduction and cortical glucose hypometabolism in DLB. We did not analyze the data on mean diffusivity, which is significantly affected by partial volume averaging of CSF. Although the influence of partial volume averaging of CSF is less on FA, up to 16% of the difference among subjects with mild cognitive impairment and CN has been attributed to macrostructural changes and associated partial volume averaging of CSF (Berlot et al., 2014). Development of robust methods for correction of partial volume averaging of CSF may improve the specificity of DTI findings in both GM and WM. Finally, we did not correct for multiple comparisons when reporting the VBA findings, which is common in AD DTI literature perhaps because of the effect sizes observed in DTI studies (Keihaninejad et al. 2012). In fact, correcting for multiple comparrissons with family-wise error correction completely diminished the group differences.

In conclusion, current data indicate that loss of parieto-occipital WM integrity is a characteristic feature of DLB, independent of AD-related Aβ deposition. This pattern of WM degeneration is consistent with the overlying reduction in glucose metabolism in the parieto-occipital cortex. Although we cannot draw inferences on any causal or temporal relationship between loss of WM and GM integrity, our findings demonstrate that microstructural changes in the WM coincide with the GM hypometabolism in the parieto-

occipital lobes in DLB patients. Longitudinal imaging studies may reveal the temporal course of GM and WM alterations in DLB.

Acknowledgements

Funding: Financial support for the conduct of the research was provided by the NIH [R01 AG040042, P50 AG016574, U01 AG06786, R01 AG11378, C06 RR018898], the Mangurian Foundation, and the Robert H. and Clarice Smith and Abigail Van Buren Alzheimer s Disease Research Program. Sponsors did not have any role in study design; in the collection, analysis and interpretation of data; in the writing of the report; and in the decision to submit the article for publication.

Y.G. is in part supported by AG-16574, Edli foundation, RWJ foundation and European Regional Development Fund-Project FNUSA-ICRC (CZ.1.05/1.1.00/02.0123). Z.N. is supported by CTSA Grant Number UL1 TR000135 from the National Center for Advancing Translational Sciences (NCATS), a component of the National Institutes of Health (NIH). Its contents are solely the responsibility of the authors and do not necessarily represent the official view of NIH; Grant Agency of Charles University in Prague (doctoral student grant 624012); by European Regional Development Fund – Project FNUSA-ICRC (CZ.1.05/1.1.00/02.0123), European Social Fund (CZ. 1.07/2.3.00/20.0117) and the State Budget of the Czech Republic.

Abbreviations

DLB	dementia with Lewy bodies
AD	Alzheimer's disease
DTI	diffusion tensor imaging
FA	fractional anisotropy
PiB PET	^{11}C Pittsburgh compound B positron emission tomography
Aβ	beta-amyloid
FDG-PET	18 F-fluorodeoxyglucose PET
CDR-SOB	Clinical Dementia Rating scale – sum of boxes
MMSE	Mini Mental State Examination
DRS	Dementia Rating Scale
VH	visual hallucinations
UPDRS	the Unified Parkinson Disease Rating Scale
pRBD	probable REM sleep behavior disorder
VBA	voxel-based analysis
SPM	statistic parametric mapping

References

AASM. International Classification of Sleep Disorders—2: Diagnostic and Coding Manual. American Academy of Sleep Medicine; Chicago: 2005.

Avants BB, Yushkevich P, Pluta J, Minkoff D, Korczykowski M, Detre J, Gee JC. The optimal template effect in hippocampus studies of diseased populations. NeuroImage. 2010; 49:2457–2466. [PubMed: 19818860]

Behrens TE, Woolrich MW, Jenkinson M, Johansen-Berg H, Nunes RG, Clare S, Matthews PM, Brady JM, Smith SM. Characterization and propagation of uncertainty in diffusion-weighted MR

imaging. Magnetic resonance in medicine : official journal of the Society of Magnetic Resonance in Medicine / Society of Magnetic Resonance in Medicine. 2003; 50:1077–1088.

Berlot R, Metzler-Baddeley, Jones DK, O'Sullivan MJ. CSF contamination contributes to apparent microstructural alterations in Mild Cognitive Impairment. Neuroimage. Feb 3.2014 2014 [e-pub].

Bozzali M, Falini A, Cercignani M, Baglio F, Farina E, Alberoni M, Vezzulli P, Olivotto F, Mantovani F, Shallice T, Scotti G, Canal N, Nemni R. Brain tissue damage in dementia with Lewy bodies: an in vivo diffusion tensor MRI study. Brain : a journal of neurology. 2005; 128:1595–1604. [PubMed: 15817515]

Bozzali M, Falini A, Franceschi M, Cercignani M, Zuffi M, Scotti G, Comi G, Filippi M. White matter damage in Alzheimer's disease assessed in vivo using diffusion tensor magnetic resonance imaging. Journal of neurology, neurosurgery, and psychiatry. 2002; 72:742–746.

Burack MA, Hartlein J, Flores HP, Taylor-Reinwald L, Perlmutter JS, Cairns NJ. In vivo amyloid imaging in autopsy-confirmed Parkinson disease with dementia. Neurology. 2010; 74:77–84. [PubMed: 20038776]

Burton EJ, Barber R, Mukaetova-Ladinska EB, Robson J, Perry RH, Jaros E, Kalaria RN, O'Brien JT. Medial temporal lobe atrophy on MRI differentiates Alzheimer's disease from dementia with Lewy bodies and vascular cognitive impairment: a prospective study with pathological verification of diagnosis. Brain : a journal of neurology. 2009; 132:195–203. [PubMed: 19022858]

Carmichael O, Lockhart S. The role of diffusion tensor imaging in the study of cognitive aging. Current topics in behavioral neurosciences. 2012; 11:289–320. [PubMed: 22081443]

Damoiseaux JS, Greicius MD. Greater than the sum of its parts: a review of studies combining structural connectivity and resting-state functional connectivity. Brain structure & function. 2009; 213:525–533. [PubMed: 19565262]

Douaud G, Jbabdi S, Behrens TE, Menke RA, Gass A, Monsch AU, Rao A, Whitcher B, Kindlmann G, Matthews PM, Smith S. DTI measures in crossing-fibre areas: increased diffusion anisotropy reveals early white matter alteration in MCI and mild Alzheimer's disease. NeuroImage. 2011; 55:880–890. [PubMed: 21182970]

Ferman TJ, Smith GE, Boeve BF, Ivnik RJ, Petersen RC, Knopman D, Graff-Radford N, Parisi J, Dickson DW. DLB fluctuations: specific features that reliably differentiate DLB from AD and normal aging. Neurology. 2004; 62:181–187. [PubMed: 14745051]

Firbank MJ, Blamire AM, Krishnan MS, Teodorczuk A, English P, Gholkar A, Harrison R, O'Brien JT. Atrophy is associated with posterior cingulate white matter disruption in dementia with Lewy bodies and Alzheimer's disease. NeuroImage. 2007; 36:1–7. [PubMed: 17412610]

Firbank MJ, Blamire AM, Teodorczuk A, Teper E, Mitra D, O'Brien JT. Diffusion tensor imaging in Alzheimer's disease and dementia with Lewy bodies. Psychiatry research. 2011; 194:176–183. [PubMed: 21955457]

Fodero-Tavoletti MT, Smith DP, McLean CA, Adlard PA, Barnham KJ, Foster LE, Leone L, Perez K, Cortes M, Culvenor JG, Li QX, Laughton KM, Rowe CC, Masters CL, Cappai R, Villemagne VL. In vitro characterization of Pittsburgh compound-B binding to Lewy bodies. The Journal of neuroscience : the official journal of the Society for Neuroscience. 2007; 27:10365–10371. [PubMed: 17898208]

Folstein MF, Folstein SE, McHugh PR. “Mini-mental state”. A practical method for grading the cognitive state of patients for the clinician. Journal of psychiatric research. 1975; 12:189–198. [PubMed: 1202204]

Foster ER, Campbell MC, Burack MA, Hartlein J, Flores HP, Cairns NJ, Hershey T, Perlmutter JS. Amyloid imaging of Lewy body-associated disorders. Movement disorders : official journal of the Movement Disorder Society. 2010; 25:2516–2523. [PubMed: 20922808]

Fujino Y, Dickson DW. Limbic lobe microvacuolation is minimal in Alzheimer's disease in the absence of concurrent Lewy body disease. International journal of clinical and experimental pathology. 2008; 1:369–375. [PubMed: 18787618]

Graff-Radford J, Murray M, Lowe VJ, Boeve BF, Ferman TJ, Przybelski SA, Lesnick TG, Senjem ML, Gunter JL, Smith GE, Knopman DS, Jack CR, Dickson DW, Petersen RC, Kantarci K. Dementia With Lewy Bodies: Basis of Cingulate Island Sign. Neurology. 2014 in press.

Higuchi M, Tashiro M, Arai H, Okamura N, Hara S, Higuchi S, Itoh M, Shin RW, Trojanowski JQ, Sasaki H. Glucose hypometabolism and neuropathological correlates in brains of dementia with Lewy bodies. Experimental neurology. 2000; 162:247–256. [PubMed: 10739631]

Huang J, Friedland RP, Auchus AP. Diffusion tensor imaging of normal-appearing white matter in mild cognitive impairment and early Alzheimer disease: preliminary evidence of axonal degeneration in the temporal lobe. AJNR. American journal of neuroradiology. 2007; 28:1943–1948. [PubMed: 17905894]

Hughes CP, Berg L, Danziger WL, Coben LA, Martin RL. A new clinical scale for the staging of dementia. The British journal of psychiatry : the journal of mental science. 1982; 140:566–572. [PubMed: 7104545]

Imamura T, Ishii K, Sasaki M, Kitagaki H, Yamaji S, Hirono N, Shimomura T, Hashimoto M, Tanimukai S, Kazui H, Mori E. Regional cerebral glucose metabolism in dementia with Lewy bodies and Alzheimer's disease: a comparative study using positron emission tomography. Neuroscience letters. 1997; 235:49–52. [PubMed: 9389593]

Jack CR Jr. Lowe VJ, Senjem ML, Weigand SD, Kemp BJ, Shiung MM, Knopman DS, Boeve BF, Klunk WE, Mathis CA, Petersen RC. 11C PiB and structural MRI provide complementary information in imaging of Alzheimer's disease and amnestic mild cognitive impairment. Brain : a journal of neurology. 2008; 131:665–680. [PubMed: 18263627]

Jellinger KA. Lewy body-related alpha-synucleinopathy in the aged human brain. Journal of neural transmission. 2004; 111:1219–1235. [PubMed: 15480835]

Jenkinson M, Beckmann CF, Behrens TE, Woolrich MW, Smith SM. Fsl. NeuroImage. 2012; 62:782–790. [PubMed: 21979382]

Kantarci K, Avula R, Senjem ML, Samikoglu AR, Zhang B, Weigand SD, Przybelski SA, Edmonson HA, Vemuri P, Knopman DS, Ferman TJ, Boeve BF, Petersen RC, Jack CR Jr. Dementia with Lewy bodies and Alzheimer disease: neurodegenerative patterns characterized by DTI. Neurology. 2010; 74:1814–1821. [PubMed: 20513818]

Kantarci K, Ferman TJ, Boeve BF, Weigand SD, Przybelski S, Vemuri P, Murray ME, Senjem ML, Smith GE, Knopman DS, Petersen RC, Jack CR Jr. Parisi JE, Dickson DW. Focal atrophy on MRI and neuropathologic classification of dementia with Lewy bodies. Neurology. 2012a; 79:553–560. [PubMed: 22843258]

Kantarci K, Lowe VJ, Boeve BF, Weigand SD, Senjem ML, Przybelski SA, Dickson DW, Parisi JE, Knopman DS, Smith GE, Ferman TJ, Petersen RC, Jack CR Jr. Multimodality imaging characteristics of dementia with Lewy bodies. Neurobiology of aging. 2012b; 33:2091–2105. [PubMed: 22018896]

Kantarci K, Yang C, Schneider JA, Senjem ML, Reyes DA, Lowe VJ, Barnes LL, Aggarwal NT, Bennett DA, Smith GE, Petersen RC, Jack CR Jr. Boeve BF. Antemortem amyloid imaging and beta-amyloid pathology in a case with dementia with Lewy bodies. Neurobiology of aging. 2012c; 33:878–885. [PubMed: 20961664]

Kiuchi K, Morikawa M, Taoka T, Kitamura S, Nagashima T, Makinodan M, Nakagawa K, Fukusumi M, Ikeshita K, Inoue M, Kichikawa K, Kishimoto T. White matter changes in dementia with Lewy bodies and Alzheimer's disease: a tractography-based study. Journal of psychiatric research. 2011; 45:1095–1100. [PubMed: 21315376]

Klunk WE, Wang Y, Huang GF, Debnath ML, Holt DP, Mathis CA. Uncharged thioflavin-T derivatives bind to amyloid-beta protein with high affinity and readily enter the brain. Life sciences. 2001; 69:1471–1484. [PubMed: 11554609]

Kramer ML, Schulz-Schaeffer WJ. Presynaptic alpha-synuclein aggregates, not Lewy bodies, cause neurodegeneration in dementia with Lewy bodies. The Journal of neuroscience : the official journal of the Society for Neuroscience. 2007; 27:1405–1410. [PubMed: 17287515]

Lee JE, Park HJ, Park B, Song SK, Sohn YH, Lee JD, Lee PH. A comparative analysis of cognitive profiles and white-matter alterations using voxel-based diffusion tensor imaging between patients with Parkinson's disease dementia and dementia with Lewy bodies. Journal of neurology, neurosurgery, and psychiatry. 2010; 81:320–326.

Mathis CA, Bacskai BJ, Kajdasz ST, McLellan ME, Frosch MP, Hyman BT, Holt DP, Wang Y, Huang GF, Debnath ML, Klunk WE. A lipophilic thioflavin-T derivative for positron emission

tomography (PET) imaging of amyloid in brain. Bioorganic & medicinal chemistry letters. 2002; 12:295–298. [PubMed: 11814781]

McKeith IG, Dickson DW, Lowe J, Emre M, O'Brien JT, Feldman H, Cummings J, Duda JE, Lippa C, Perry EK, Aarsland D, Arai H, Ballard CG, Boeve B, Burn DJ, Costa D, Del Ser T, Dubois B, Galasko D, Gauthier S, Goetz CG, Gomez-Tortosa E, Halliday G, Hansen LA, Hardy J, Iwatsubo T, Kalaria RN, Kaufer D, Kenny RA, Korczyn A, Kosaka K, Lee VM, Lees A, Litvan I, Londos E, Lopez OL, Minoshima S, Mizuno Y, Molina JA, Mukaetova-Ladinska EB, Pasquier F, Perry RH, Schulz JB, Trojanowski JQ, Yamada M. Diagnosis and management of dementia with Lewy bodies: third report of the DLB Consortium. Neurology. 2005; 65:1863–1872. [PubMed: 16237129]

McKhann G, Drachman D, Folstein M, Katzman R, Price D, Stadlan EM. Clinical diagnosis of Alzheimer's disease: report of the NINCDS-ADRDA Work Group under the auspices of Department of Health and Human Services Task Force on Alzheimer's Disease. Neurology. 1984; 34:939–944. [PubMed: 6610841]

Medina D, DeToledo-Morrell L, Urresta F, Gabrieli JD, Moseley M, Fleischman D, Bennett DA, Leurgans S, Turner DA, Stebbins GT. White matter changes in mild cognitive impairment and AD: A diffusion tensor imaging study. Neurobiology of aging. 2006; 27:663–672. [PubMed: 16005548]

Meltzer CC, Kinahan PE, Greer PJ, Nichols TE, Comtat C, Cantwell MN, Lin MP, Price JC. Comparative evaluation of MR-based partial-volume correction schemes for PET. Journal of nuclear medicine : official publication, Society of Nuclear Medicine. 1999; 40:2053–2065.

Mesulam MM. From sensation to cognition. Brain: a journal of neurology. 1998; 121:1013–52. [PubMed: 9648540]

Middelkoop HA, van der Flier WM, Burton EJ, Lloyd AJ, Paling S, Barber R, Ballard C, McKeith IG, O'Brien JT. Dementia with Lewy bodies and AD are not associated with occipital lobe atrophy on MRI. Neurology. 2001; 57:2117–2120. [PubMed: 11739838]

Mielke MM, Kozauer NA, Chan KC, George M, Toroney J, Zerrate M, Bandeen-Roche K, Wang MC, Vanzijl P, Pekar JJ, Mori S, Lyketsos CG, Albert M. Regionally-specific diffusion tensor imaging in mild cognitive impairment and Alzheimer's disease. NeuroImage. 2009; 46:47–55. [PubMed: 19457371]

Minoshima S, Foster NL, Sima AA, Frey KA, Albin RL, Kuhl DE. Alzheimer's disease versus dementia with Lewy bodies: cerebral metabolic distinction with autopsy confirmation. Annals of neurology. 2001; 50:358–365. [PubMed: 11558792]

Morris JC. The Clinical Dementia Rating (CDR): current version and scoring rules. Neurology. 1993; 43:2412–2414. [PubMed: 8232972]

Murray ME, Ferman TJ, Boeve BF, Przybelski SA, Lesnick TG, Liesinger AM, Senjem ML, Gunter JL, Preboske GM, Lowe VJ, Vemuri P, Dugger BN, Knopman DS, Smith GE, Parisi JE, Silber MH, Graff-Radford NR, Petersen RC, Jack CR Jr. Dickson DW, Kantarci K. MRI and pathology of REM sleep behavior disorder in dementia with Lewy bodies. Neurology. 2013

Nedelska Z, Ferman TJ, Boeve BF, Przybelski SA, Lesnick TG, Murray ME, Gunter JL, Senjem ML, Vemuri P, Smith GE, Geda YE, Graff-Radford J, Knopman DS, Petersen RC, Parisi JE, Dickson DW, Jack CR Jr. Kantarci K. Pattern of brain atrophy rates in autopsy-confirmed dementia with Lewy bodies. Neurobiology of aging. 2014

Ota M, Sato N, Saitoh Y, Endo F, Murata M, Asada T. Diffusion tensor imaging in familial spastic paraplegia with mental impairment and thin corpus callosum. Magnetic resonance in medical sciences : MRMS : an official journal of Japan Society of Magnetic Resonance in Medicine. 2008; 7:163–167.

Pierpaoli C, Basser PJ. Toward a quantitative assessment of diffusion anisotropy. Magnetic resonance in medicine : official journal of the Society of Magnetic Resonance in Medicine / Society of Magnetic Resonance in Medicine. 1996; 36:893–906.

Rowe CC, Ng S, Ackermann U, Gong SJ, Pike K, Savage G, Cowie TF, Dickinson KL, Maruff P, Darby D, Smith C, Woodward M, Merory J, Tochon-Danguy H, O'Keefe G, Klunk WE, Mathis CA, Price JC, Masters CL, Villemagne VL. Imaging beta-amyloid burden in aging and dementia. Neurology. 2007; 68:1718–1725. [PubMed: 17502554]

Salat DH, Tuch DS, van der Kouwe AJ, Greve DN, Pappu V, Lee SY, Hevelone ND, Zaleta AK, Growdon JH, Corkin S, Fischl B, Rosas HD. White matter pathology isolates the hippocampal formation in Alzheimer's disease. Neurobiology of aging. 2010; 31:244–256. [PubMed: 18455835]

Schwarz CG, Reid RI, Gunter JL, Senjem ML, Przybelski SA, Zuk SM, Whitwell JL, Vemuri P, Josephs KA, Kantarci K, Thompson PM, Petersen RC, Jack CR Jr. Improved DTI registration allows voxel-based analysis that outperforms Tract-Based Spatial Statistics. NeuroImage. 2014; 94:65–78. [PubMed: 24650605]

Tzourio-Mazoyer N, Landeau B, Papathanassiou D, Crivello F, Etard O, Delcroix N, Mazoyer B, Joliot M. Automated anatomical labeling of activations in SPM using a macroscopic anatomical parcellation of the MNI MRI single-subject brain. NeuroImage. 2002; 15:273–289. [PubMed: 11771995]

Vemuri P, Gunter JL, Senjem ML, Whitwell JL, Kantarci K, Knopman DS, Boeve BF, Petersen RC, Jack CR Jr. Alzheimer's disease diagnosis in individual subjects using structural MR images: validation studies. NeuroImage. 2008; 39:1186–1197. [PubMed: 18054253]

Watson R, Blamire AM, Colloby SJ, Wood JS, Barber R, He J, O'Brien JT. Characterizing dementia with Lewy bodies by means of diffusion tensor imaging. Neurology. 2012; 79:906–914. [PubMed: 22895591]

Whitwell JL, Weigand SD, Shiung MM, Boeve BF, Ferman TJ, Smith GE, Knopman DS, Petersen RC, Benarroch EE, Josephs KA, Jack CR Jr. Focal atrophy in dementia with Lewy bodies on MRI: a distinct pattern from Alzheimer's disease. Brain : a journal of neurology. 2007; 130:708–719. [PubMed: 17267521]

Zaja-Milatovic S, Keene CD, Montine KS, Leverenz JB, Tsuang D, Montine TJ. Selective dendritic degeneration of medium spiny neurons in dementia with Lewy bodies. Neurology. 2006; 66:1591–1593. [PubMed: 16717229]

Highlights

- Dementia with Lewy bodies is characterized by a loss of parieto-occipital white matter integrity independent of β-amyloid load.
- Microstructural changes in the white matter topographically coincide with the gray matter hypometabolism in the parieto-occipital lobes in patients with dementia with Lewy bodies.
- The temporal course of gray matter and white matter alterations in dementia with Lewy bodies require further investigation.

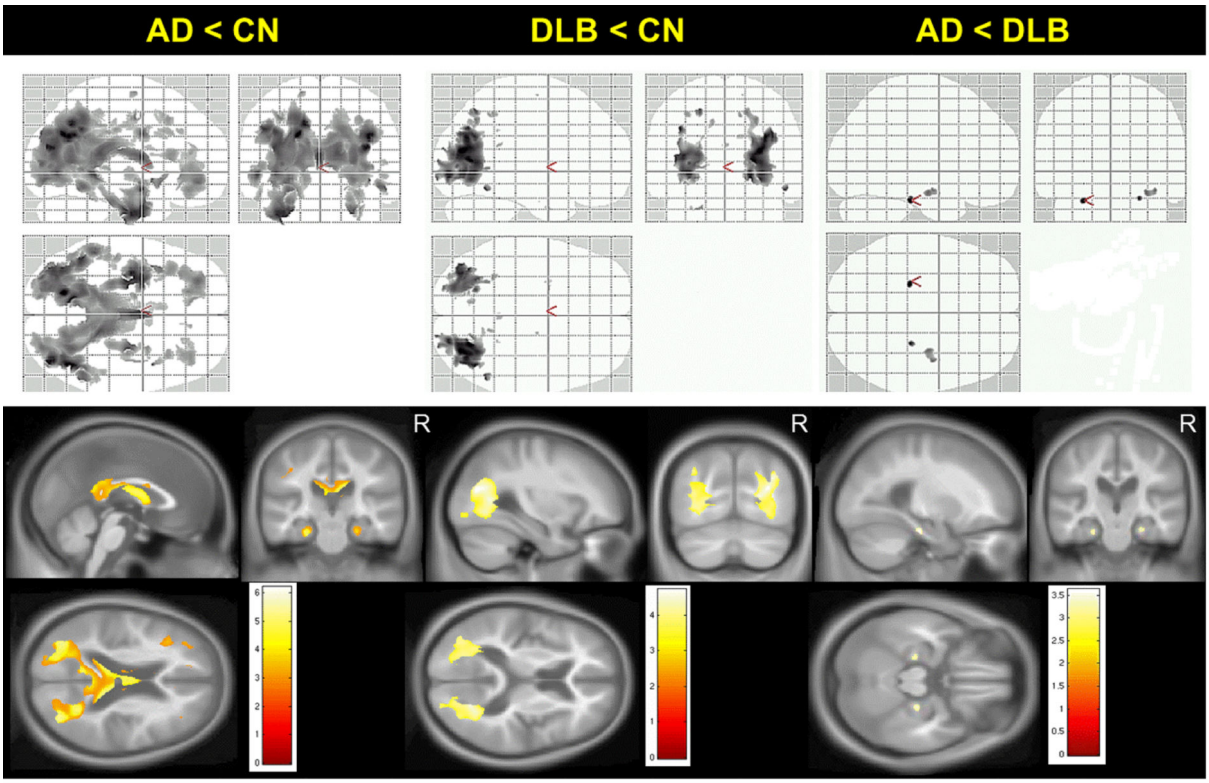

Figure 1. Patterns of differences in FA between clinical groups on voxel-based analysis

Voxel-level maps show topographic pattern of between-group differences in FA. FA maps overlaid on glass brain from SPM (top row) or anatomical sections (bottom row) show magnitude of the differences in FA using side T-statistic bars, $p<0.001$(uncorrected). AD patients have wide-spread FA decreases in temporo-parietal, occipital and frontal white matter compared to CN (left column). DLB patients have reduced FA confined to parieto-occipital white matter compared to CN (middle column). In AD, reduced FA in parahippocampal white matter is observed compared to DLB patients (right column).

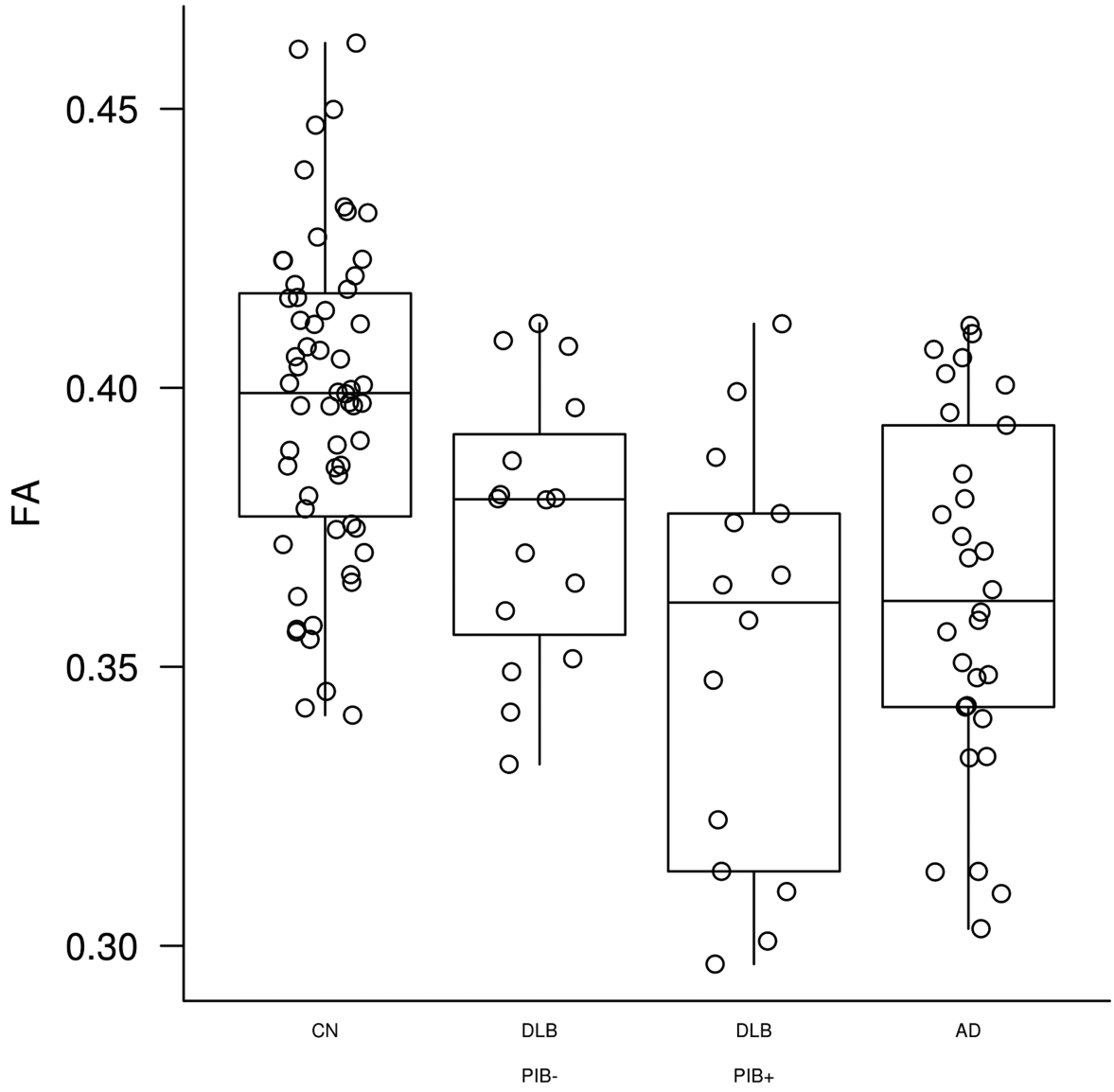

Figure 2. Parieto-occipital FA in PiB positive and PiB negative DLB

FA values from VBA-derived WM regions, where FA was significantly reduced in DLB compared to CN are displayed in PiB positive (SUVR<1.5) and PiB negative (SUVR≥1.5) DLB subjects compared to AD and CN subjects.

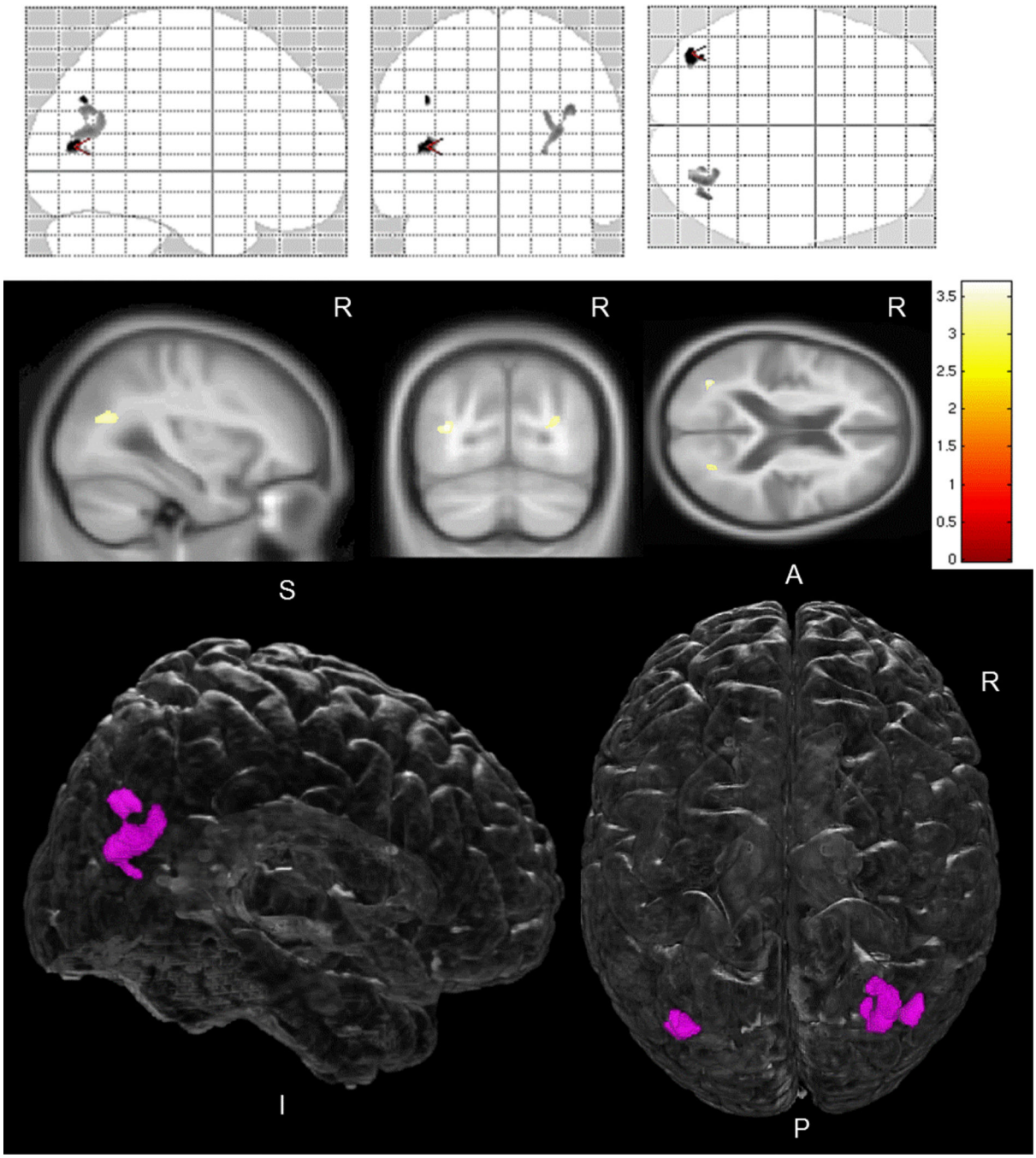

Figure 3. Pattern of reduced FA in DLB patients compared to CN, adjusted for Aβ load

Voxel-level maps show pattern of reduced FA in DLB patients compared to CN. FA maps overlaid on glass brain from SPM (top row) or anatomical sections (middle row) show magnitude of the FA differences between these two groups using side T-bars, $p<0.001$(uncorrected) on voxel-based analysis. Bottom row shows FA differences overlaid on a 3D glass-brain render from MRIcroGL (http://www.mccauslandcenter.sc.edu/mricrogl/), with FA decreases confined to a well circumscribed region in parieto-occipital white matter.

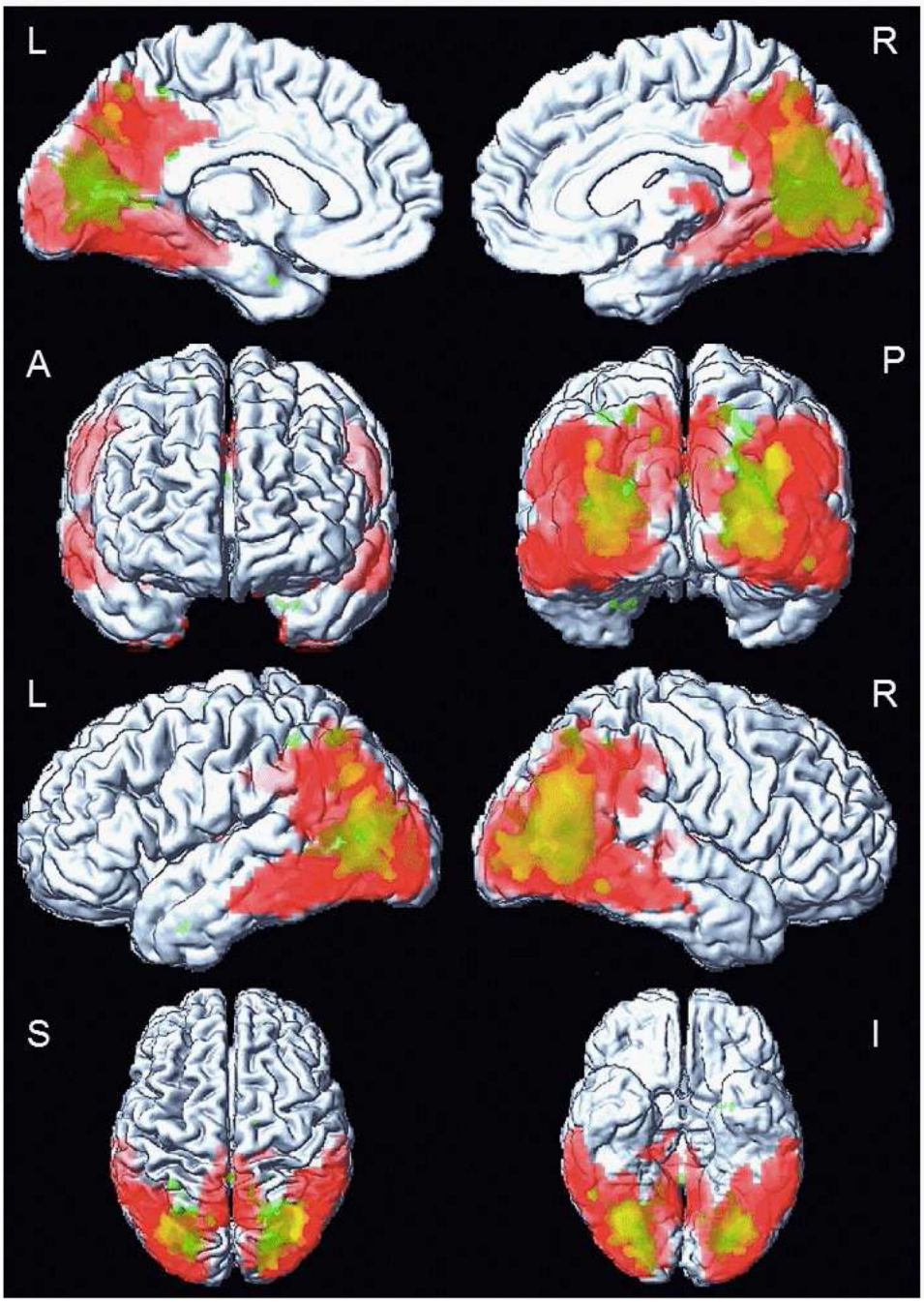

Figure 4. Overlapping patterns of white matter and cortical grey matter alterations in DLB patients on voxel-based analysis

Cortical glucose hypometabolism on 18F-FDG PET is overlapping with reduced FA in white matter on DTI in DLB patients compared to CN. The overlap is displayed on a surface render using SPM5. The white matter alteration (green color) is confined to parieto-occipital region, $p<0.001$ (uncorrected). The alteration in cortical glucose metabolism (red color) is more diffuse, in posterior temporal, parietal and in occipital cortices, $p<0.001$, (FWE corrected).

Table 1

Subjects' characteristics.

	CN n = 60	DLB n = 30	AD n = 30	p-value*
Females (%)	10 (17)	5 (17)	5 (17)	1.0
Age (y)	68.5 (63, 76)	69 (63, 76)	72.5 (64, 79)	0.48
Education (y)	15.5 (12.5, 18)	15 (12, 18)	16 (12, 18)	0.69
APOE ε4 carriers (%)	11 (18)	13 (43)	23 (77)	<0.001
CDR sum of boxes	0.0 (0.0, 0.0)	5.75 (4.0, 7.0)	4.75 (2.5, 7.0)	<0.001
MMSE	29 (28, 29)	20.5 (15, 24)	21 (14, 23)	<0.001
DRS	-	125.5 (114, 131)	111 (85, 127)	0.03
PiB SUVR	1.31 (1.27, 1.37)	1.43 (1.30, 1.88)	2.35 (2.17, 2.52)	<0.001
VH present (%)	-	23 (77)	2 (8)	<0.001
Fluctuations present (%)	-	27 (90)	2 (8)	<0.001
Motor UPDRS	-	12 (7, 14)	0 (0, 2)	<0.001
RBD present (%)	-	28 (93)	4 (15)	<0.001
Dementia duration (y)	-	5.04 (3.75, 7.17)	5.21 (3.50, 7.00)	0.88
VH duration (y)	-	1.91 (0.75, 3.59)	-	-
Fluctuations duration (y)	-	2.25 (1.49, 3.67)	-	-
Parkinsonism duration (y)	-	3.50 (1.17, 5.75)	-	-
RBD duration (y)	-	9.21 (4.16, 14.08)	-	-

Medians (IQR) are listed for the continuous and the proportions (%) are for the categorical variables.

*p-values are from the Wilcoxon rank sum for the continuous variables, and a χ^2 test for differences in proportions. VH = visual hallucinations (probable and definite combined together). RBD = probable REM-sleep behavior disorder, SUVR=Standardized uptake value ratio.